Calculating Sputter Rate Angular Dependence Using Optical Profilometry

IEPC-2007-001

Presented at the 30th International Electric Propulsion Conference, Florence, Italy
September 17-20, 2007

Alexander C. Barrie* and Bryan S. Taylor†
Advatech Pacific. Inc., Palmdale, CA, 93550, United States

and

Jared M. Ekholm‡ and William H. Hargus§
Air Force Research Laboratory, 1 Ara Rd., Edwards AFB, CA, United States

Abstract: This work attempts to determine angular dependence curves for sputter rates of a material based on a single experimental measurement. An aluminum cylinder was exposed to a BHT-200 plume and the resulting erosion profile was measured. This profile was fed into an optimizer, which calculated the angular dependence curve to match the given erosion profile. The calculated profile matched well with the experimental profile, however neither matched well will previously published results. The likely cause of this discrepancy was the non-uniformity of the ion source used. As a further validation of the optimization routine, the angular dependence curve was input to the Coliseum plasma modeling code, which generated the same erosion profile as the experimental data.

Nomenclature

Y	= sputter yield
E	= incident ion energy
$Q, \alpha^*, \Sigma, s, f, \theta_{opt}$	= empirical sputter curve fit parameter
M_1	= ion mass
M_2	= surface particle mass
S_n	= nuclear stopping power
U_s	= sublimation energy
Γ	= mechanism B-sputtering contribution
k_e	= Lindhard electronic stopping coefficient
ϵ	= reduced energy
dx	= erosion depth
Φ	= particle flux
N_A	= Avagadro's number
ρ_s	= surface material density
T	= time multiplier

*Aerospace Engineer, Space and Missiles Division, alex.barrie@advatechpacific.com
†Aerospace Engineer, Space and Missiles Division, bryan.taylor@advatechpacific.com
‡Research Engineer, PRSS, jared.ekholm@us.af.mil.
§Research Engineer, PRSS, william.hargus@edwards.af.mil.

I. Introduction

SURFACE sputtering and erosion are of paramount concern for missions utilizing electric propulsion (EP) based thrusters. Typical ion energies from EP thrusters can be in the hundreds of eV. Impingement of ions on a surface can cause substantial sputtering of the surface material. Surface sputtering can cause deposition onto optics, degradation of thermal systems, changes to electrical properties, and, in some cases, structural deformation. Several previous works have focused on single event ion sputtering and prediction. Boyd[1] presents a literature review of the current state of sputter prediction. Surface sputtering is highly dependent on the incident ion impact angle, and will therefore change over time as a given surface erodes.

Sputter rates can not always be easily obtained from compiled data. New composites, alloys, or uncommon materials may not have data available. Additionally, environmental factors, such as plasma sheaths, can alter the expected sputtering behavior of a material. This work presents a new method for calculating the angular dependence of the sputter yield based on the erosion profile of a known reference cylinder.

A 0.25 inch aluminum cylinder was exposed to a BHT-200[2,3] plume for a period of 72 hours. The erosion profile was then measured using an optical profilometer. A computational optimizer was used to calculate the angular dependence of the sputter yield curve. To validate this angular dependence, the Coliseum[4] plasma modeling package was then used to replicate the profile of the eroded cylinder.

Coliseum is a framework consisting of several plasma simulation packages developed by the Air Force Research Lab, Advatech Pacific, and several universities and industries. This paper focuses on the Draco[5] package, a fully kinetic/hybrid ES-PIC routine. Draco utilizes a stretched Cartesian volume mesh intersected by a triangulated surface mesh. An erosion module has been added to the Draco code allowing for surface sputtering, redeposition, and the deformation of a surface over long time intervals.

Draco surfaces are composed of triangulated meshes. As particles impact a surface element, a sputter yield value is calculated and weighed onto each of the three nodes making up the element. At a user specified interval, the nodes are moved according the the accumulated erosion value. Nodes are moved along normal vectors formed by averaging the normal direction of all adjacent surface elements.

II. Experimental Setup

These experiments were conducted in Chamber 6 located at the Air Force Research Laboratory (AFRL) Electric Propulsion Laboratory at Edwards AFB, CA. Chamber 6 measures 1.8 m in diameter and 3.0 m in length with a pumping speed of 32,000 l/s of xenon using four single stage cryopanels and one 50 cm dual stage cryopump. During nominal chamber operations chamber pressure is approximately 6×10^{-6} Torr, corrected for xenon.

The Busek Co, Inc. BHT-200 xenon Hall thruster was used in this experiment. The BHT-200 produces 12 mN of thrust at a system efficiency of 35% while operating at nominal discharge voltages and conditions, see Table 1.

For the purpose of this experiment, an aluminum alloy 6061 rod measuring 0.25 inches in diameter was used. Prior to plume exposure the rod was sandblasted to ensure a uniform surface texture and remove any oxidation. An 16 mm test section was identified for plume impingement. Adjacent to this section, Kapton tape was wrapped around the rod to protect a small area of the rod from the plume and provide a ready reference to measure the quantity of material eroded.

Optical profilometry measurements were performed to establish a pre-erosion baseline. The profilometer used was a STIL Micromeasure measurement system with a STIL CHR contactless optical sensor capable of 1 micron resolution. The available profilometry software cannot control a rotation stage, so a series of planar scans were taken in 30° increments controlled by a manual rotation stage.

The long axis of the rod was placed perpendicular to the thruster 10.7 cm downstream of the nose cone and aligned 90° to the thruster. It was grounded to the chamber wall. The rod was exposed to the thruster plume for a period of 72 hours. At the termination of the period the rod was again removed and profiled. The profilometry and chamber setups are shown in Figure 1.

Anode Flow	840 μg/s (Xe)
Cathode Flow	98 μg/s (Xe)
Anode Potential	250 V
Anode Current	0.85 A
Heater Current	3.0 A
Keeper Current	0.5 A
Magnet Current	0.75 A

Table 1. Typical operating conditions of the Busek BHT-200 Hall thruster.

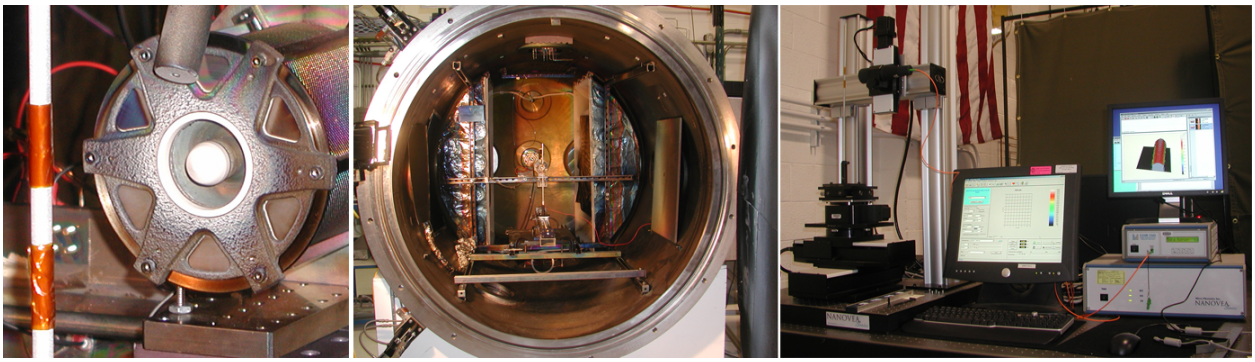

Figure 1. Aluminum rod and thruster in chamber (left and center). Profilometer with mounted rod (right).

III. Algorithms

A. Erosion

Surface erosion is calculated using the sputter yield and particle flux to a surface. Surface nodes are moved at user defined intervals based on the accumulated sputter. The sputter yield from the experimental results was obtained by converting a distance into an molecular yield.

$$Y = \frac{dx N_A \rho_s}{\Phi M_2 T} \tag{1}$$

where Φ is the particle flux, M_2 is the molecular mass of the surface material, and ρ_s is the density of the surface material. For a typical plasma simulation, erosion rates are on a much larger timescale than plasma parameters. For this reason, a time multiplier, T, is applied to the erosion rate.

B. Sputter Yield

There are several algorithms to calculate sputter yield.[6–10] This study used the Yamamura yield model. The Yamamoura normal yield is given by

$$Y(E) = 0.042 \frac{Q\alpha^*(M_2/M_1)Sn(E)}{U_s(1+\Gamma k_e \epsilon^{0.3})} \times \left[1 - \sqrt{\frac{E_{th}}{E}}\right]^s \tag{2}$$

where E is the incident energy and all other terms are material constants and empirical fit factors. Yamamura[6] presents a complete explanation and derivation of terms. For this study, an average normal yield was obtained using average flux and measured erosion at normal incidence. This average normal yield was then given as an input to the optimizer. The Yamamura angular dependance[11] is given by

$$Y(\theta) = Y(0)\cos^{-f}\theta e^{-\Sigma(\cos^{-1}\theta - 1)} \tag{3}$$

θ_{opt} then relates Σ and f.

$$\cos(\theta_{opt}) = \frac{\Sigma}{f} \tag{4}$$

C. Determination of Sputter Yield Angular Dependance

Typically, a series of experiments is performed impinging a flat plate with ions of varying incidence to gain an overall angular dependence curve for sputter yields. Given an eroded cylinder profile, the angular sputter yield dependence and normal sputter yield of the material can be determined in a single measurement. As shown in Equation 3, the angular dependence of the sputter yield for a given material and incident particle flux can be determined by two constants: f and Σ. An optimizer can be used to determine these constants by matching calculated erosion profiles with a measured experimental profile, thus obtaining the complete angular dependence curve using only one experimental measurement. A code was written to deform a cylinder over time using the Yamamura sputter yield. A uniform, monoenergetic flux was assumed. After a user specified time, the resulting profile is compared to a given profile using a least squares method for a variety of input states. This process is repeated with increasingly fine input resolution and narrow input range until an optimum solution is reached.

IV. Experimental Results

A 0.25 *in* aluminum cylinder was placed in a BHT-200 plume and allowed to erode for a period of 72 hours. The resulting surface profile was measured with an optical profilometer and compared to the initial profile. The resulting change in profile was fed into an optimizer and Yamamura constants were calculated to match the erosion rates attained.

The eroded cylinder is shown in Figure 2. Figures 3 and 4 show the measured profile. The degree increments correspond to the measured profiles in Figure 5 and the millimeter increments correspond to the measured profiles in Figure 6.

Figure 5 shows the erosion profile after 72 hours. The profiles are non-uniform due to a non-ideal plasma environment. There is a central bulge indicating less erosion near the center (8 mm) than near the taped area (0 mm). This may be because the tape itself affected the plasma. Kapton is a dielectric and may have charged to a non-zero potential. A potential gradient near the taped area could have accounted for a variable particle flux along the length of the exposed area.

There is also a higher erosion level towards the left side (0 mm, see Fig. 6) of the exposed area. This is likely due to the rod not being perfectly aligned with the centerline of the thruster. The exposed area was placed as close to the centerline of the thruster as was possible, but this does not guarantee alignment in the plume.

Thruster plumes are not always focused directly over the centerline and there may have been a small rotation in the thruster mounting causing off-center impingement. Significant erosion is shown to have occurred at 90° and a small amount of erosion as far as 120°. This is due to the overall erosion of the surface. As the surface erodes, the point on the surface at 90° from the thruster is no longer the point of maximum horizontal distance. This is shown in Figure 4.

The cross sectional erosion profile is shown in Figure 6 along with the average total erosion over the three measurements and the baseline, uneroded profile. A slight non-uniformity is present. The profile near the taped area has a higher erosion rate at higher angles and a lower erosion rate near normal incidence than the centerline (0 degree) profile. Again, this may have been caused by effects related to the Kapton tape. This nonuniformity is shown more clearly in Figure 7.

The centerline (8 mm) profile was input to the optimizer and Yamamura constants were determined for the described erosion profile. A resulting contour plot of the error in the least squares fit is shown in Figure 8. For graphical reasons, the maximum value was capped at 100 and undefined values are shown as 0. A line of local minima is present in the contour. This line represents a profile where the normal erosion and the high angle erosion are the most accurate. As the line of local minima itself lowers to an absolute minimum, the erosion profile begins to match more closely in the intermediate angle value range. For this case, optimum values were found to be 1.1 for f and 0.1 for Σ.

The calculated values for f and Σ did not match the expected values. Based on published[11] material and empirical constants, aluminum exposed to 200 eV ions should have an f of 8.6 and a Σ of 4.3. In Figure 8 these values lie in the bottom of the trough representing local minima, however are not the absolute

Figure 2. Aluminum rod before exposure (left) followed by 72 hour erosion photos ranging from -90 degrees to +90 degrees from incidence.

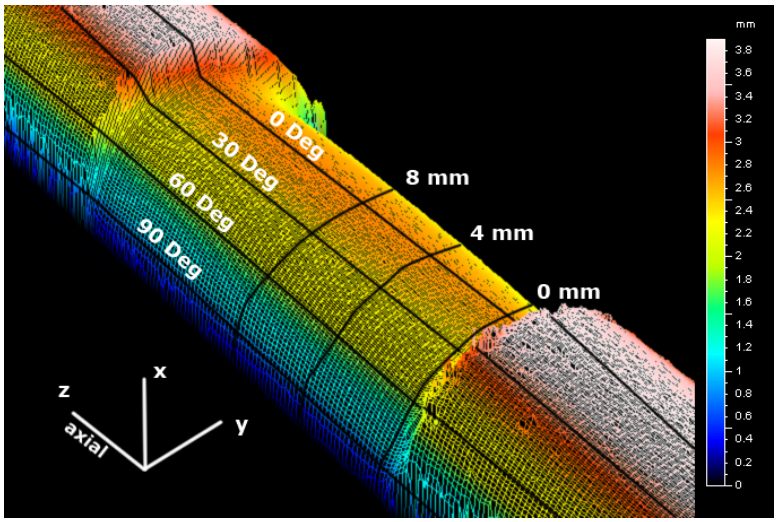

Figure 3. Erosion profile at normal incidence after 72 hours. Lines are shown as reference for future plots.

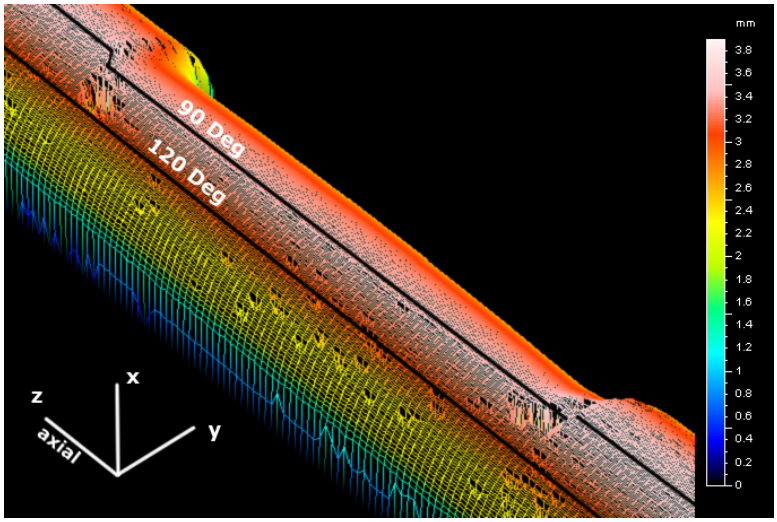

Figure 4. Erosion profile at 90° from incidence after 72 hours. Lines are shown as reference for future plots.

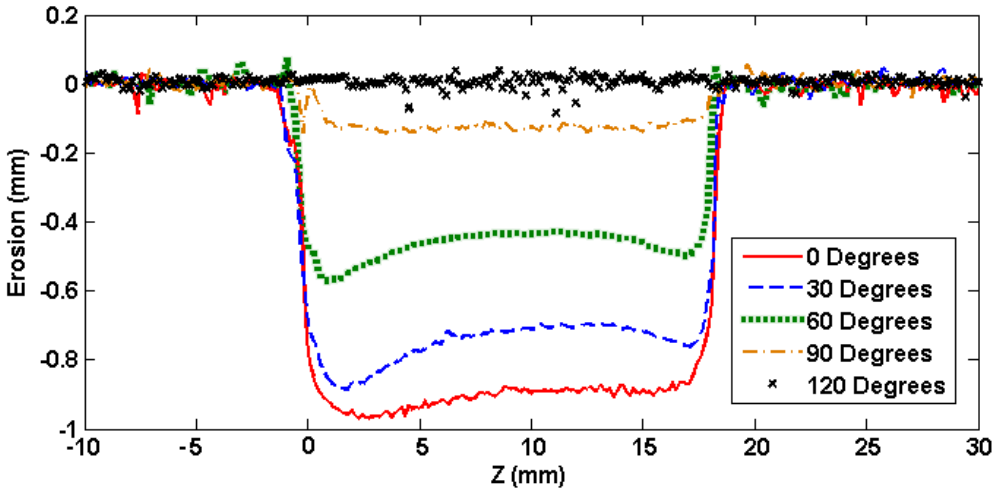

Figure 5. Erosion profile in the axial direction at varying positions on the rod (See Fig. 3).

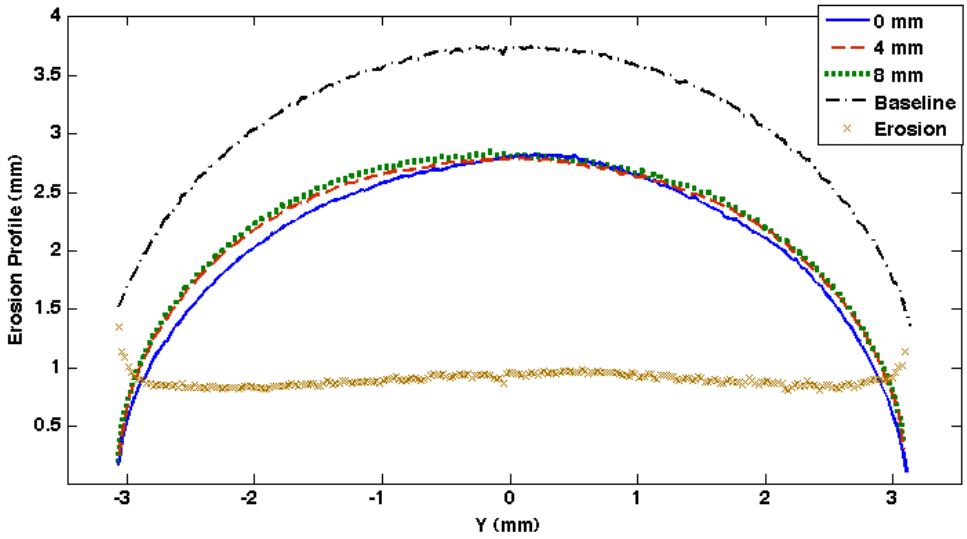

Figure 6. Erosion profile of cross section at varying positions on the rod (See Fig. 3).

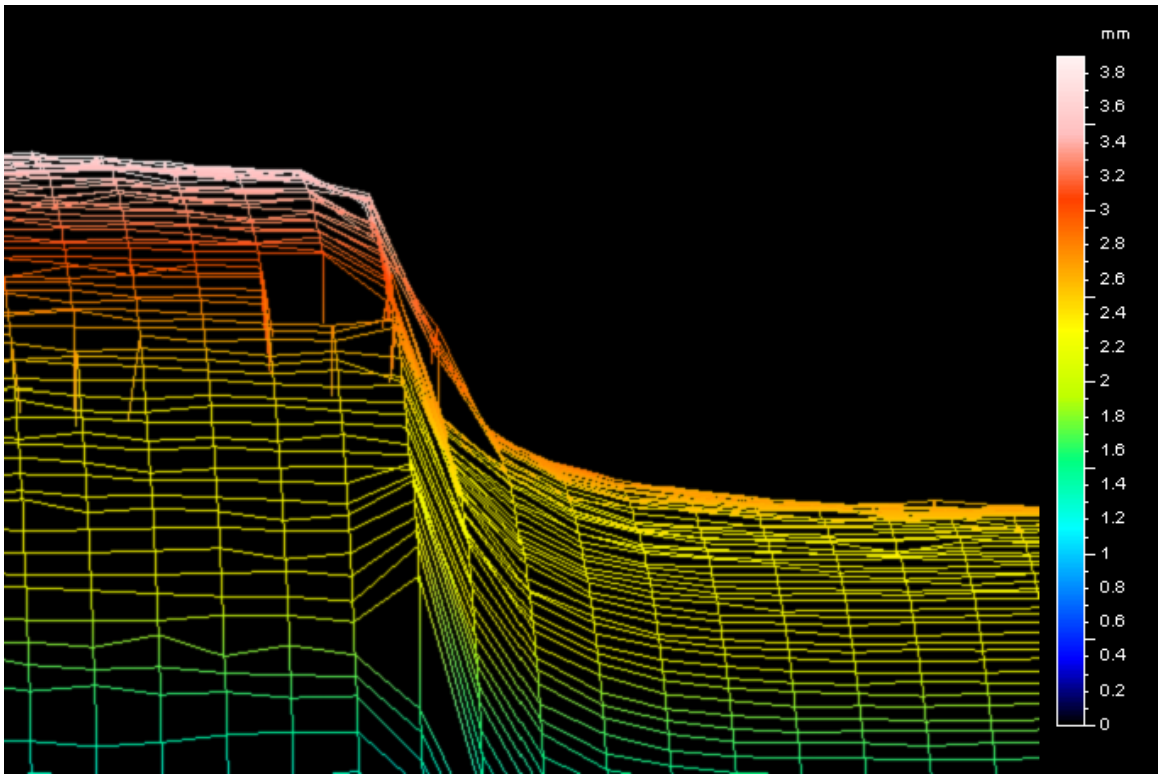

Figure 7. Transition between eroded section and protected section of rod.

minimum values. This implies that the erosion near 0 and 90 degrees is correct, however the intermediate values are not correct.

As points move down the line of local minima towards a Σ value of 0, the erosion profile becomes more circular with a weaker angular dependance for small angles and a larger angle dependency at high angles. Larger values tend to have a stronger angular dependency at smaller angles. This difference is shown in Figure 9. The published Yamamura constants for aluminum yield a dependence curve with a maximum yield around 60°. The calculated constants represent a maximum yield of similar magnitude, but at 80°. A flatter dependence curve, or one where the peak is at a high angle, will result in a relatively uniform erosion profile. Dependence curves with peaks further from 90 degrees result in sharper erosion profiles, such as the Yamamura aluminum line shown in Figure 10.

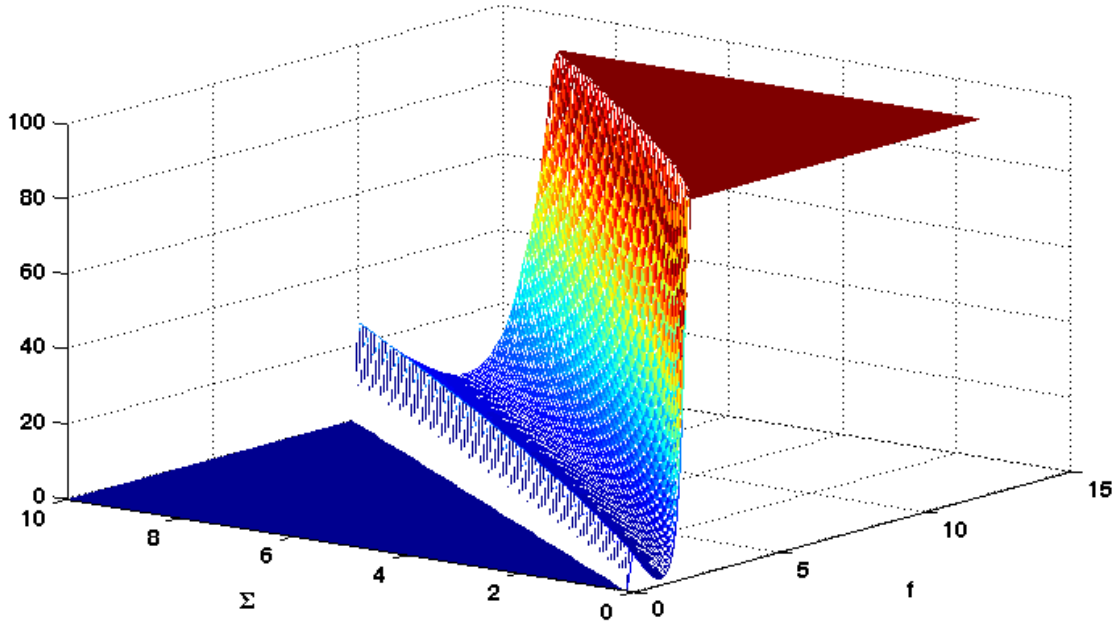

Figure 8. Surface mesh showing least squares fit of Yamamura constants.

Figure 10 shows that the calculated inputs for Yamamura match the experimental profile well, but neither the calculated constants, nor the experimental profile, match up to the profile resulting from the published values for aluminum. The unexpected erosion profile is likely due to the plasma source. The calculations performed assumed a mono-energetic, uniform, 200 eV plasma. The BHT-200 was thought to be an adequate approximation, but this may not have been correct.

Measurements of the BHT-200 plume[2,3] show three distinct populations: singly charged ions, doubly charged ions, and triply charged ions. These are in addition to electrons and neutral xenon particles. None of these species are mono-energetic, but are instead described by maxwellian distributions. Furthermore, Hall thrusters have beam divergence, collisions, and field effects that cause non axial velocity components to develop.

Additional effects may have taken place as a result of the rod itself. The plasma potential[2,3] was several volts above the ground voltage which may have caused a plasma sheath to form around the cylinder. This plasma sheath would act to redirect some ions towards the rod, altering the incident angle. While this effect may adversely affect the attempt to replicate the published Yamamura numbers, plasma sheaths will often develop in real world environments. For this reason, this technique may be useful for predicting sputter behavior where plasma sheaths may be present, such as with probes.

In future experiments it should be advantageous to use a more suitable ion source. Gridded ion thrusters have more columnated, mono-energetic beams and are being considered. The test sample should also be matched as closely as possible with the local plasma potential to avoid any sheathing effects.

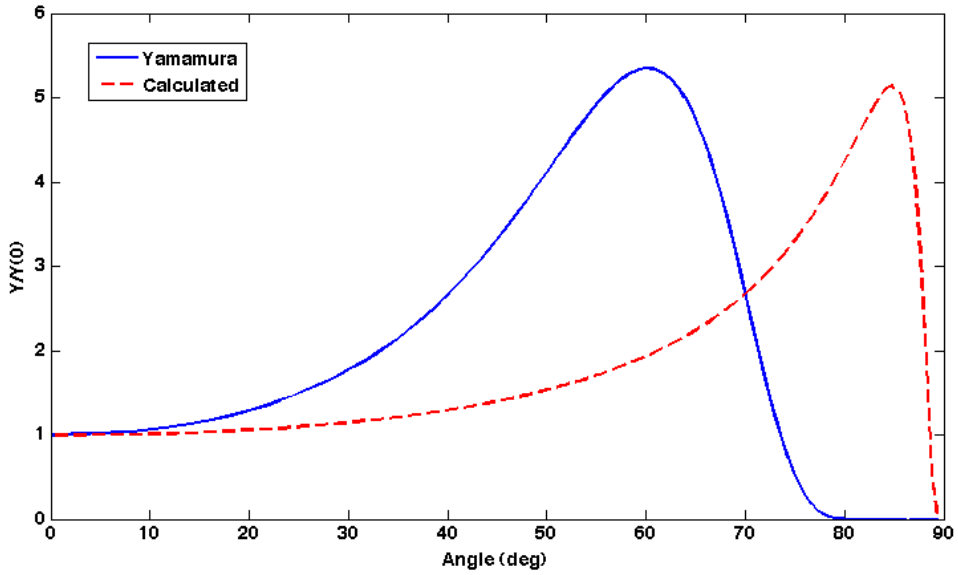

Figure 9. Angular dependence curves based on calculated constants and published Yamamura values.

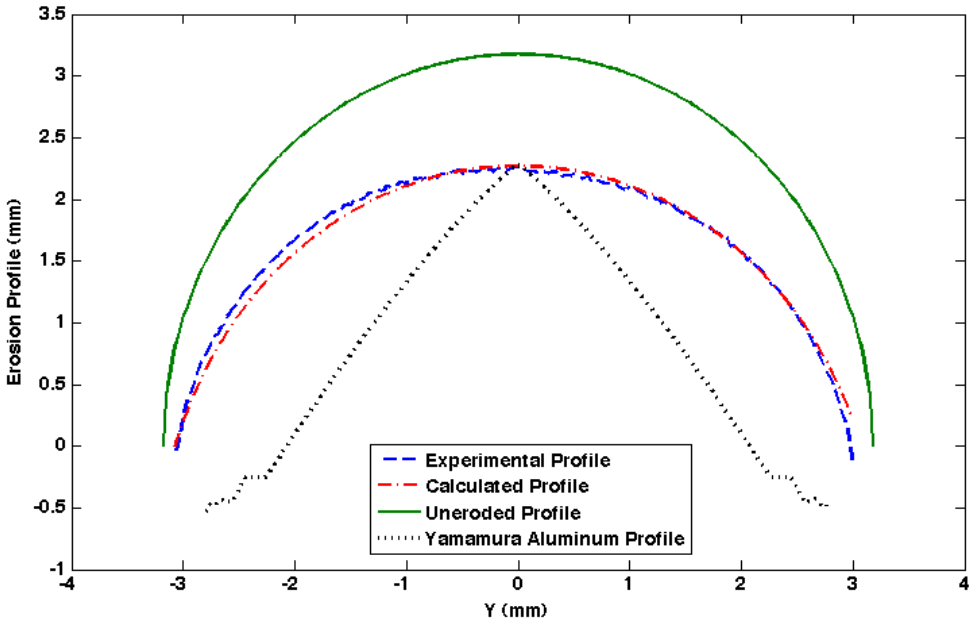

Figure 10. Erosion profiles compared with Yamamura value.

V. Coliseum Validation

A. Simulation Setup

The Coliseum code was used to simulate the erosion of a 0.25 *in* aluminum cylinder. The domain consisted of a $60 \times 60 \times 60$ grid of $0.2mm$ cells, for a total domain size of 12 $mm \times 12$ $mm \times 12$ mm. A 0.25 *in* cylinder consisting of 40 radial partitions and 20 axial partitions was inserted into the center of the domain. The simulation setup is shown in Figure 11. The cylinder extends vertically out of the domain to eliminate edge effects from the simulation.

The simulation was run for 10,000 timesteps of 2e-9 seconds. The erosion was calculated every 100 timesteps. Through use of the erosion rate multiplier, the total erosion time simulated was 72 hours. A plasma with properties given in Table 2 was injected from one side of the domain to replicate the plasma flux from the BHT-200 plume. Coliseum can simulate a BHT plume with reasonable accuracy,[3] however this study used a uniform plasma to replicate the idealized input conditions to the optimizer rather than the physical experimental plume.

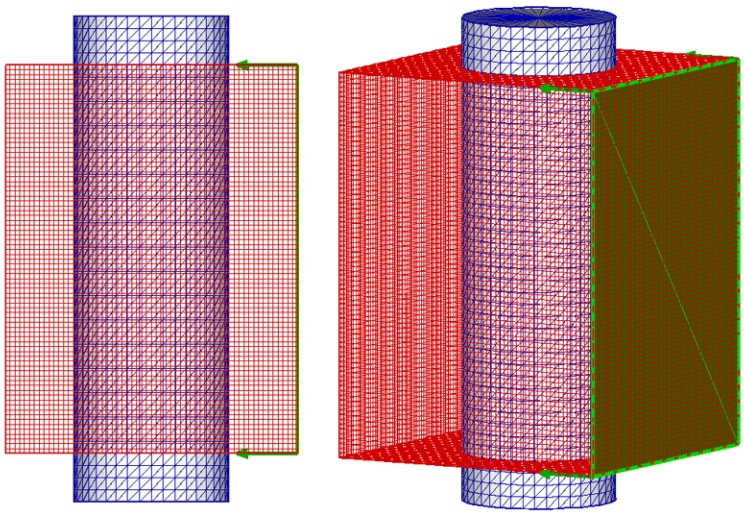

Figure 11. Simulation domain used by Coliseum. Particle source shown in green.

Plasma Parameters		
Specie Parameters		
$s1$	Ion specie	Xe+
$s2$	Target specie	Al
$\dot{m}$	Mass flow rate	1E-6 (kg/s)
v	Ion exit velocity	16,800 (m/s)
T	Ion temperature	1,000 (K)

Table 2. Plasma source and material parameters used by Coliseum.

B. Results

Coliseum was used to further validate the erosion optimization routine. The erosion profile is shown in Figure 12 along with the experimental and optimizer profile. The Coliseum profile matches well with the profile from the optimizer. This makes sense as the calculated Yamamura values from the optimizer were used for the Coliseum calculation. This shows that when sheathing effects and a non-uniform plasma source are present, the sputter rates and the resulting erosion profile can still be predicted with accuracy using this method.

Similar to Figure 2, Figure 13 shows the eroded cylinder computed by Coliseum. This allows for a three dimensional view of the erosion profile rather than the two dimensional view from the optimizer. The area of transition between the eroded area and the area protected by the kapton tape is not resolved as well in the Coliseum simulation. This is because of the cell sizing of the surface mesh. Erosion of cells is split among that cells nodes based on distance from the impact point. Any node that is a member of a cell that is eroded will receive some erosion. It is therefore difficult to resolve effects smaller than one cell width, such as a taped edge. This effect can be mitigated by having a reduced cell size.

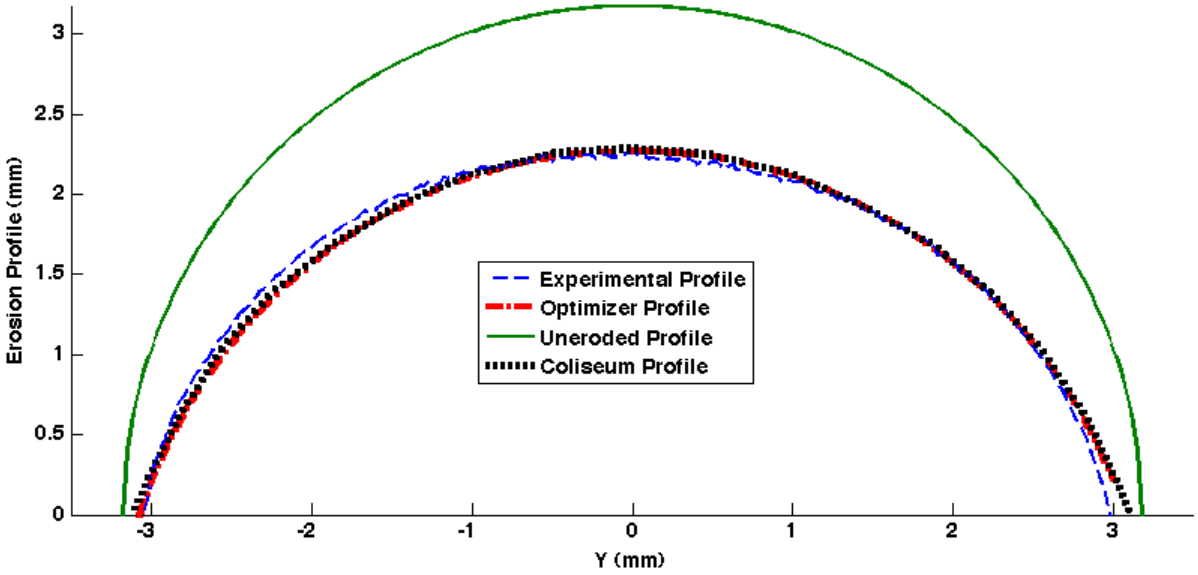

Figure 12. Coliseum erosion profiles compared with Yamamura profile and profile as calculated by optimizer along the center of the eroded area.

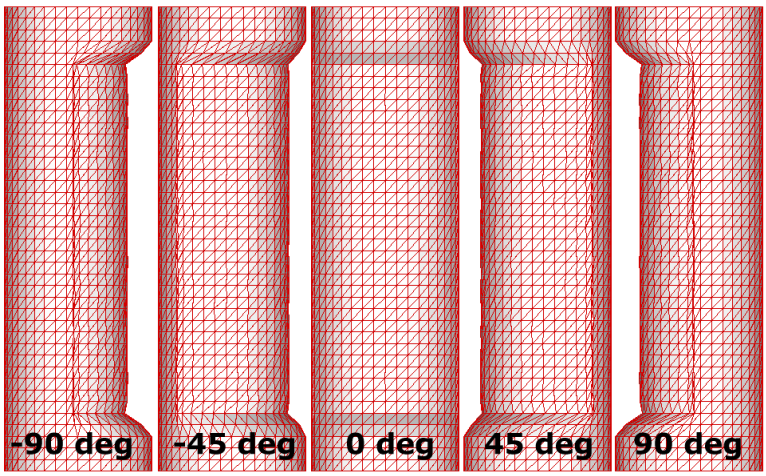

Figure 13. Eroded cylinder from Coliseum simulation.

VI. Future Work

This study presents a proof of concept for a method of measuring sputter yield angular dependence. Although the method and algorithms generated erosion profiles and dependence curves that matched the experimental data, the experimental data did not match published values. Additional erosion tests will be performed using a more uniform ion source, such as a gridded ion thruster. A detailed characterization of

the plasma source will be required. Future improvements will also include attempting to match the rod potential with the plasma potential, and using a conductive tape instead of kapton.

Once the experimental setup is perfected, a variety of materials need to be tested including metals and nonmetals. Current plans are to test graphite and molybdenum. If this methodology proves accurate for well known materials, it can then be tested for largely unknown materials such as composites.

Common configurations that have substantial plasma effects can also be tested. This would include plasma probes, ion optics, dielectric materials, etc. Having sputter coefficients that account for known plasma variations would eliminate the need model the nuances of the plasma and surface interaction in sputtering calculations.

VII. Conclusion

Surface sputtering is a phenomenon that removes material from a surface by way of particle impingement. This effect is dependent on particle energy, incidence angle, and material properties. Current methods are limited to measuring sputtering at a single energy and angle of incidence resulting in many required experiments to fully characterize a given material. This work demonstrates a new technique to measure the angular sputter yield dependence for a given material in a single measurement.

An aluminum cylinder was exposed to a BHT-200 plume and allowed to erode for a period of 72 hours. The resulting profile was measured using an optical profilometer and compared to the initial, uneroded, shape. The erosion profile was fed into an optimization routine that used a least squares method to determine optimal constants for use in the Yamamura angular dependence function for sputter yields. Constants were calculated that resulted in a close match between the calculated erosion profile and the experimental profile.

Although the calculated profile matched well to the experiment, neither profile was consistent with published data. The likely cause of this is the ion source used. Hall effect thrusters do not emit a uniform plasma, as per the assumptions. Further effects from the sheath formed around the probe may also have been present. Future studies should be conducted to determine if this method will obtain the correct dependence curves given a mono-energetic, columnated ion source. If a controlled test case can be achieved, accurate sputter yield angular dependence curves can be obtained with a single measurement instead of the individual measurements per angle that are currently required.

These plasma effects are common in many situations, however, and this technique may be useful for modeling sputter rates when these phenomena are present. In order to use the published sputter yields in these types of situations, the exact behavior of the plasma and surface interactions must be factored into the sputter yield equation. This technique eliminates that need by calculating the sputter yield with all field effects included.

Coliseum has a variety of plasma solving routines and now has a surface erosion routine. The erosion constants obtained from the optimizer can be used in Coliseum to model erosion of uncharacterized materials. This module can be used to model erosion on a variety of real world surfaces where erosion may be an issue. Particularly in cases with unique shapes, materials, and redeposition concerns, Coliseum will be a useful tool in predicting sputtering, redeposition, and surface erosion patterns.

References

[1]Boyd, I. D. and Falk, M. L., "A Review of Spacecraft Material Sputtering by Hall Thruster Plumes," *37th AIAA/ASME/SAE/ASEE Joint Propulsion Conference and Exhibit*, 2001.

[2]Ekholm, J. M. and Hargus, W. A., "E×B Measurements of a 200 W Xenon Hall Thruster," *41st AIAA/ASME/SAE/ASEE Joint Propulsion Conference and Exhibit*, 2005.

[3]Nakles, M. R. and et. al., "Experimental and Numerical Examination of the BHT-200 Hall Thruster Plume," *43rd AIAA/ASME/SAE/ASEE Joint Propulsion Conference and Exhibit*, 2007.

[4]Fife, J. and et. al., "The Development of a Flexible, Usable Plasma Interaction Modeling System," *38th AIAA/ASME/SAE/ASEE Joint Propulsion Conference and Exhibit*, July 2002.

[5]Breida, L., Kafafy, R., Pierru, J., and Wang, J., "Development of the DRACO Code for Modeling Electric Propulsion Plume Interactions," *40th AIAA/ASME/SAE/ASEE Joint Propulsion Conference and Exhibit*, July 2004.

[6]Yamamura, Y. and Tawara, H., "Energy Dependence of Ion Induced Sputtering Yields From Monatomic Solids at Normal Incidence," *Atomic Data and Nuclear Tables*, Vol. 62, 1996.

[7]Kannenberg, K. and et. al., "Validation of Hall Thruster Plume Sputter Model," *37th AIAA/ASME/SAE/ASEE Joint Propulsion Conference and Exhibit*, 2001.

[8]Zhang, Z. L. and Zhang, L., "Anisotropic Angular Distributions of Sputtered Atoms," *Radiation Effects and Defects in Solids*, Vol. 159, 2004.

[9]Yalin, A. P. and et. al., "Differential Sputter Yield Profiles of Molybdenum due to Bombardment by Low Energy Xenon Ions at Normal and Oblique Incidence," *Submitted to: Journal of Physics D: Applied Physics*.

[10]Anderson, H. H., "Computer Simulations of Atomic Collisions in Solids with Special Emphasis on Sputtering," *Nuclear Instruments and Methods in Physics Research*, Vol. B18, 1987.

[11]Yamamura, Y., "An Empirical Formula for Angular Dependence of Sputtering Yields," *Radiation Effects*, Vol. 80, 1984.